Progress In Electromagnetics Research, PIER 20, 101–123, 1998

ANALYSIS OF ELECTROMAGNETIC SCATTERING OF CONDUCTING CIRCULAR DISK USING A HYBRID METHOD

L. W. Li, P. S. Kooi, Y. L. Qiu, T. S. Yeo, and M. S. Leong

Communications & Microwave Division
Dept. of Electrical Engineering
National University of Singapore
10 Kent Ridge Crescent, Singapore 119260

1. Introduction
2. Eigenfunctional Expansions of Electromagnetic Fields
3. Analysis Using Hybrid Method
4. Scattered Electromagnetic Fields
5. Backscattering Cross Section
6. Numerical Discussion
7. Conclusions
Acknowledgment
References

1. INTRODUCTION

Over several decades, electromagnetic (EM) scattering from a circular disk has attracted researchers with a strong interest in the (monostatic or backscattering) radar cross sections (RCS's) of large dynamic range. Usually, as reviewed by Duan and Rahmat-Samii [1], the following groups of techniques are applied to the analysis of the electromagnetic scattering from circular disks.

The first type is the physical optics (PO) [2] which is an approximate technique and is accurate for predicting the far-field pattern near the main beam. The second type is the physical theory of diffraction (PTD) [3] which is more accurate than the PO technique since the equivalent edge current is applied and the caustic singularities in the

original ray tracing are eliminated. This method is further modified (a) by Ando [4] using equivalent edge currents, (b) by Mitzner [5] utilizing the incremental length diffraction coefficients, and (c) by Michaeli [6, 7] using surface–to–edge integral and the fringe current radiation integral over the *ray coordinates* instead of the *normal coordinates* (also see [8]). the third type is the geometrical theory of Diffraction (GTD) [9–13] that is of similar accuracy to the PTD. This method was also modified into (a) uniform geometrical theory of diffraction by Kouyoumijian and Pathak [14], (b) uniform asymptotic technique by Ahluwalia et al. [15] and Lee & Deschamps [16], and (c) High–Order Geometrical Theory of Diffraction by Bechtel [17] and Ryan & Peters [18] (of the 1st order), by Knott et al. [19] (of the second order), and by Marsland et al. [20] (of the higher–orders). The fourth type is the method of moments (MoM) or moment method (MM) [1] that is considered to be numerically exact. The Hybrid Asymptotic Moment Method is implemented by Kim and Thiele first who found the induced currents on the scatterer surface. This method was further modified by Kaye, Murthy and Thiele [21, 22], and thus the fifth type of methods was formed, i.e., the hybrid–iterative method which employs the magnetic field integral equation for the induced currents to solve the scattering problems.

This paper presents a novel analysis of the classical electromagnetic scattering problem, i.e., EM scattering from a conducting circular disk. A hybrid method which combines the vector wave eigenfuction expansion technique, the least squares technique, the mode-matching method, and the dyadic Green's function is applied to the derivative of the unknown scattering coefficients of the expanded eigenfuctions of the scattered fields. This method is similar to the MoM and therefore has the same order of accuracy as the MoM. Orthogonality of the vector wave functions is partially utilized. The scattering coefficients are obtained and expressed in terms of compact matrices. Numerical computation of the radar cross sections of the perfectly conducting disk is carried out and found to be faster than that in the Moment Method. Experimental data and theoretical results published elsewhere are compared with the results obtained in this paper. A good agreement in the comparison confirms the applicability of the hybrid method developed in this paper.

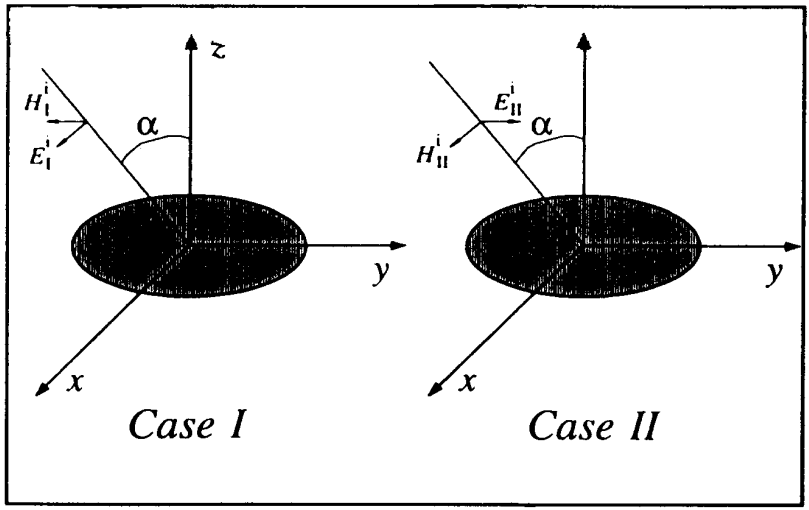

Figure 1. Geometry of plane waves scattered by a conducting circular disk.

2. EIGENFUCTIONAL EXPANSIONS OF ELECTROMAGNETIC FIELDS

Consider the geometry shown in Fig. 1 where an incident plane electromagnetic wave is scattered by a perfectly conducting circular disk.

Two pairs of incident EM waves are used to account for parallel (I) and perpendicular (II) polarizations in this paper. They are expressed by:

$$\boldsymbol{E}_I^i = E_I \,(\cos\,\alpha\hat{\boldsymbol{x}} - \sin\,\alpha\hat{\boldsymbol{z}})\, e^{ik_0(x\sin\alpha + z\cos\alpha)} \tag{1a}$$

$$\boldsymbol{H}_I^i = \frac{k_0\, E_I}{\omega\mu_0}\,\hat{\boldsymbol{y}}\, e^{ik_0(x\sin\alpha + z\cos\alpha)} \tag{1b}$$

and

$$\boldsymbol{E}_{II}^i = E_{II}\,\hat{\boldsymbol{y}}\, e^{ik_0(x\sin\alpha + z\cos\alpha)} \tag{2a}$$

$$\boldsymbol{H}_{II}^i = -\frac{k_0\, E_{II}}{\omega\mu_0}\,(\cos\alpha\hat{\boldsymbol{x}} - \sin\alpha\hat{\boldsymbol{z}})\, e^{ik_0(x\sin\alpha + z\cos\alpha)} \tag{2b}$$

It is assumed for convenience that the incident wave lies on the $\hat{\boldsymbol{x}}\hat{\boldsymbol{z}}$-plane, i.e., $\phi' = 0$.

These two polarized incident EM fields in (1) and (2) can be expanded in terms of vector wave eigenfunctions defined in the spherical coordinates system as follows:

$$\begin{aligned}
\boldsymbol{M}_{\substack{e\\o}mn}(k) = &\mp \frac{mz_n(kr)}{\sin\theta} P_n^m(\cos\theta) \begin{matrix}\sin\\\cos\end{matrix} m\phi\,\hat{\boldsymbol{\theta}} \\
&- z_n(kr)\frac{\partial P_n^m(\cos\theta)}{\partial\theta} \begin{matrix}\cos\\\sin\end{matrix} m\phi\,\hat{\boldsymbol{\phi}} \\
\boldsymbol{N}_{\substack{e\\o}mn}(k) = &\frac{n(n+1)z_n(kr)}{kr} P_n^m(\cos\theta) \begin{matrix}\cos\\\sin\end{matrix} m\phi\hat{\boldsymbol{r}} \\
&+ \frac{\partial[rz_n(kr)]}{kr\partial r} \frac{\partial P_n^m(\cos\theta)}{\partial\theta} \begin{matrix}\cos\\\sin\end{matrix} m\phi\,\hat{\boldsymbol{\theta}} \\
&\mp \frac{m}{\sin\theta} \frac{\partial[rz_n(kr)]}{kr\partial r} P_n^m(\cos\theta) \begin{matrix}\sin\\\cos\end{matrix} m\phi\,\hat{\boldsymbol{\phi}}
\end{aligned}$$

where $z_n(kr)$ represents the spherical Bessel functions of n-order, and $P_n^m(\cos\theta)$ is the associated Legendre function.

The incident waves under the two polarizations have, as introduced by Morrison and Cross [23], the following forms:

$$\boldsymbol{E}_{\substack{I\\II}}^i = \sum_{n=1}^{\infty}\sum_{m=0}^{n}\left[a_{\substack{e\\o}mn}^i \boldsymbol{M}_{\substack{o\\e}mn}(k_0) + b_{\substack{o\\e}mn}^i \boldsymbol{N}_{\substack{e\\o}mn}(k_0)\right] \tag{4a}$$

$$\boldsymbol{H}_{\substack{I\\II}}^i = \frac{ik_0}{\omega\mu_0}\sum_{n=1}^{\infty}\sum_{m=0}^{n}\left[a_{\substack{e\\o}mn}^i \boldsymbol{N}_{\substack{o\\e}mn}(k_0) + b_{\substack{e\\o}mn}^i \boldsymbol{M}_{\substack{e\\o}mn}(k_0)\right] \tag{4b}$$

where the spherical Bessel functions of the first kind, i.e., $z_n(k_0r) = j_n(k_0r)$, are used in the above vector wave functions, the orthogonal properties of $\boldsymbol{M}_{\substack{e\\o}mn}(k_0)$ and $\boldsymbol{N}_{\substack{e\\o}mn}(k_0)$ are considered, and the coefficients of the expanded incident EM fields, $a_{\substack{e\\o}mn}^i$ and $b_{\substack{e\\o}mn}^i$ are given by

$$a_{\substack{o\\e}mn}^i = (2-\delta_{m0})\,i^n\,\mathcal{N}_{nm}\begin{Bmatrix}\frac{mP_n^m(\cos\alpha)}{\sin\alpha}E_I\\ -\frac{\partial P_n^m(\cos\alpha)}{\partial\alpha}E_{II}\end{Bmatrix}, \tag{5a}$$

$$b_{\substack{e\\o}mn}^i = -(2-\delta_{m0})\,i^{n+1}\,\mathcal{N}_{nm}\begin{Bmatrix}\frac{\partial P_n^m(\cos\alpha)}{\partial\alpha}E_I\\ \frac{mP_n^m(\cos\alpha)}{\sin\alpha}E_{II}\end{Bmatrix}, \tag{5b}$$

where δ_{mn} ($=1$ for $m=n$; and 0 for $m\neq n$) denotes the Kronecker symbol and $\mathcal{N}_{nm}$ is the normalization coefficient given by

$$\mathcal{N}_{nm} = \frac{(2n+1)}{n(n+1)}\frac{(n-m)!}{(n+m)!}. \tag{6}$$

To solve for the unknown scattered field, the following well-known integrals of scattered fields excited by the surface current distribution $\boldsymbol{J}_s$ in free-space are recommended:

$$\boldsymbol{E}^s_{\substack{I\\II}} = i\omega\mu_0 \iint_A \overline{\boldsymbol{G}}_{EJ0}(\boldsymbol{r},\boldsymbol{r}')\cdot \boldsymbol{J}^s_{\substack{I\\II}}(\boldsymbol{r}')dS' \tag{7a}$$

$$\boldsymbol{H}^s_{\substack{I\\II}} = \iint_A \nabla\times\overline{\boldsymbol{G}}_{EJ0}(\boldsymbol{r},\boldsymbol{r}')\cdot \boldsymbol{J}^s_{\substack{I\\II}}(\boldsymbol{r}')dS' \tag{7b}$$

where the subscript A represents the area of the conducting circular disk, $\overline{\boldsymbol{G}}_{EJ0}(\boldsymbol{r},\boldsymbol{r}')$ denotes the dyadic Green's function of the electric kind in free space, and $\boldsymbol{J}^s_{\substack{I\\II}}(\boldsymbol{r}')$ represents the surface current distribution on the disk. The subscript $\substack{I\\II}$ used denotes the parallel (I) and perpendicular (II) polarized wave excitations.

The dyadic Green's function of the electric kind in free space wave given earlier in terms of the spherical vector wave functions by Tai [24] and applied by Li et al. [25] recently. It is written as

$$\overline{\boldsymbol{G}}_{EJ0}(\boldsymbol{r},\boldsymbol{r}') = -\frac{\hat{\boldsymbol{r}}\hat{\boldsymbol{r}}}{k_0^2}\delta(\boldsymbol{r}-\boldsymbol{r}') + \frac{ik_0}{4\pi}\sum_{n=1}^{\infty}\sum_{m=0}^{n}(2-\delta_{m0})\mathcal{N}_{nm}$$
$$\cdot\begin{cases} \boldsymbol{M}^{(1)}_{\substack{e\\o}mn}(k_0)\boldsymbol{M}'_{\substack{e\\o}mn}(k_0) + \boldsymbol{N}^{(1)}_{\substack{e\\o}mn}(k_0)\boldsymbol{N}'_{\substack{e\\o}mn}(k_0), & r\geq r'\ ; \\ \boldsymbol{M}_{\substack{e\\o}mn}(k_0)\boldsymbol{M}'^{(1)}_{\substack{e\\o}mn}(k_0) + \boldsymbol{N}_{\substack{e\\o}mn}(k_0)\boldsymbol{N}'^{(1)}_{\substack{e\\o}mn}(k_0), & r\leq r'. \end{cases} \tag{8}$$

It is to be noted that the notations $\substack{e\\o}mn$ and $\substack{o\\e}mn$ of the dyadic Green's function in (8) have a different meaning from those in (4)-(5) where the upper (or lower) notation denotes the I parallel (or the II perpendicular) polarization. Here in (8), it means the summation form of both even and odd modes should be taken into account when the integrals in (7) are evaluated. Thus, when the Green's function in (7) is integrated, positions of the upper and lower notations emn and omn can be exchanged.

Clearly, we can solve the problem easily if the surface current distribution is known. To obtain the surface current distribution, different approaches are employed, as briefly reviewed in the Introduction section. Among those approaches, some of them assumed approximate equivalent edge currents, but the Method of Moments is considered to be a numerically exact technique which expands the current distribution into a series of assumed and known basis functions. Once

these expansion coefficients are determined by matching the boundary conditions for the electric fields on the conducting surface, the surface current distribution can be obtained, from which the scattered electric field can be evaluated using (7). This method has been well-documented by Harrington [26, 27] and has also been applied by Duan et al. [1].

In this paper, we proposed a new hybrid method for solving this scattering problem. As we know, the PO surface current on the patch can be obtained by using

$$\underset{II}{\boldsymbol{J}_I^{PO}} = 2\hat{n} \times \underset{II}{\boldsymbol{H}_I^i}(\boldsymbol{r}') = -2\,\hat{\boldsymbol{\theta}} \times \underset{II}{\boldsymbol{H}_I^i}(\boldsymbol{r}'), \tag{9}$$

where the incident magnetic field is given by (4b). In an explicit form, the $\hat{\boldsymbol{r}}$-component and $\hat{\boldsymbol{\theta}}$ component are expressed by

$$\begin{aligned}
\underset{II}{\boldsymbol{J}_I^{PO,r}} =& -\frac{i2k_0}{\omega\mu_0}\sum_{m=0}^{\infty}\left\{\begin{bmatrix}\cos\\ \sin\end{bmatrix}(m\phi')\right] \\
&\cdot\sum_{n=m}^{\infty}(1-\delta_{n0})\left[\pm\underset{e}{\overset{i}{a_o}}_{mn}\frac{\partial[r' j_n(k_0 r')]}{k_0 r'\partial r'}\,mP_n^m(0)\right. \\
&\left.-\underset{o}{\overset{i}{b_e}}_{mn}\,j_n(k_0 r')\,\frac{\partial P_n^m(0)}{\partial\theta}\right]\Bigg\}, \qquad (10a)\\
\underset{II}{\boldsymbol{J}_I^{PO,\phi}} =& \frac{i2k_0}{\omega\mu_0}\sum_{m=1}^{\infty}\left[\begin{matrix}\sin\\ \cos\end{matrix}(m\phi')\right] \\
&\cdot\sum_{n=m}^{\infty}(1-\delta_{n0})\left[\underset{e}{\overset{i}{a_o}}_{mn}\frac{n(n+1)j_n(k_0 r')}{k_0 r'}P_n^m(0)\right]. \qquad (10b)
\end{aligned}$$

It should be pointed out that the following relationships exist

$$\begin{aligned}
P_n^m(0) &= 0, \qquad n+m \text{ odd},\\
\frac{dP_n^m(0)}{d\theta} &= 0, \qquad n+m \text{ even}.
\end{aligned}$$

In principle, the radial component of the electric current almost vanishes at the edge which the azimuth component of the electric current becomes almost infinity at the edge [9]. Thus we may assume, based on the PO electric current, a modified form of the electric current with

the following components:

$$\begin{aligned}\boldsymbol{J}^{r}_{\substack{I\\II}} =& -\frac{i2k_0}{\omega\mu_0}\begin{bmatrix}1\\0\end{bmatrix}\cdot\sum_{n=1}^{\infty}\Bigg[\pm a^{i}_{\substack{o\\e}0n}\frac{\partial[r'j_n(k_0r')]}{k_0r'\partial r'}P_n^0(0)\\ &\qquad\qquad - b^{i}_{\substack{e\\o}0n}\,j_n(k_0r')\,\frac{\partial P_n^0(0)}{\partial\theta}\Bigg]\\ &-\frac{i2k_0}{\omega\mu_0}\sum_{m=1}^{\infty}\Bigg\{A^{m}_{\substack{I\\II}}\sqrt{1-p\left(\frac{r'}{a}\right)^2}\begin{bmatrix}\cos\\ \sin\end{bmatrix}(m\phi')\Bigg]\\ &\cdot\sum_{n=m}^{\infty}\left[\pm a^{i}_{\substack{o\\e}mn}\frac{\partial[r'j_n(k_0r')]}{k_0r'\partial r'}\,mP_n^m(0) - b^{i}_{\substack{e\\o}mn}\,j_n(k_0r')\,\frac{\partial P_n^m(0)}{\partial\theta}\right]\Bigg\},\end{aligned} \tag{11a}$$

$$\begin{aligned}\boldsymbol{J}^{\phi}_{\substack{I\\II}} =& \frac{i2k_0}{\omega\mu_0}\begin{bmatrix}0\\1\end{bmatrix}\cdot\sum_{n=1}^{\infty}\left[a^{o}_{\substack{e\\e}0n}\frac{n(n+1)j_n(k_0r')}{k_0r'}P_n^0(0)\right]\\ &+\frac{i2k_0}{\omega\mu_0}\sum_{m=1}^{\infty}\Bigg\{\frac{B^{m}_{\substack{I\\II}}}{\sqrt{1-p\left(\frac{r'}{a}\right)^2}}\begin{bmatrix}\sin\\ \cos\end{bmatrix}(m\phi')\Bigg]\\ &\cdot\sum_{n=m}^{\infty}\left[a^{i}_{\substack{o\\e}mn}\frac{n(n+1)j_n(k_0r')}{k_0r'}P_n^m(0)\right]\Bigg\}\end{aligned} \tag{11b}$$

where $A^{m}_{\substack{I\\II}}$ and $B^{m}_{\substack{I\\II}}$ $(m=1,2,\cdots)$ are two coefficient vectors to be determined.

3. ANALYSIS USING HYBRID METHOD

To determine the two unknown coefficients, the boundary conditions on the patch surface must be employed. The conditions in vector form are given as follows:

$$\hat{\boldsymbol{\theta}}\times\left(\boldsymbol{E}^{i}_{\substack{I\\II}}+\boldsymbol{E}^{s}_{\substack{I\\II}}\right)=0. \tag{12}$$

Apparently, the left-hand side of (12) is a function of radial distance r and angle ϕ. If the Method of Moments is applied, we used to multiply the weighting function (or the basis function in the Galerkin's method) to the both sides of (12) and to integrate them over the spatial domain region. In a similar fashion, here we multiply both the left and right

hand sides of (12) by $\begin{matrix}\cos\\ \sin\end{matrix}(m\phi)$ and integrate them over 0 to 2π. We then have

$$A^m_{\substack{I\\II}}\,\eta^A_{m^I_{II}}(r_i)+B^m_{\substack{I\\II}}\,\eta^B_{m^I_{II}}(r_i)=\chi_{m^I_{II}}(r_i), \tag{13a}$$

$$A^m_{\substack{I\\II}}\,\xi^A_{m^I_{II}}(r_i)+B^m_{\substack{I\\II}}\,\xi^B_{m^I_{II}}(r_i)=\tau_{m^I_{II}}(r_i), \tag{13b}$$

where the six coefficients $\eta^A_{m^I_{II}}(r_i)$, $\eta^B_{m^I_{II}}(r_i)$, $\xi^A_{m^I_{II}}(r_i)$, $\xi^B_{m^I_{II}}(r_i)$, $\chi_{m^I_{II}}(r_i)$, and $\tau_{m^I_{II}}(r_i)$ at a particular point $r=r_i$ ($i=1,2,\cdots,N$ and N is the number of the discrete points) are given by

$$\begin{aligned}\eta^A_{m^I_{II}}(r_i)=&-\frac{ik_0^2}{2}\begin{bmatrix}1+\delta_{m0}\\1-\delta_{m0}\end{bmatrix}\sum_{n=m}^{\infty}[n(n+1)P_n^m(0)]^2\\&\times\left\{\frac{h_n^{(1)}k_0r_i}{k_0r_i}\sum_{n'=m}^{\infty}\left[\pm\mathcal{C}^2_{(m,n')^I_{II}}(r_i)-\mathcal{C}^3_{(m,n')^I_{II}}(r_i)\right]\right.\\&\left.+\frac{j_n(k_0r_i)}{k_0r_i}\sum_{n'=m}^{\infty}\left[\pm\mathcal{D}^2_{(m,n')^I_{II}}(r_i)-\mathcal{D}^3_{(m,n')^I_{II}}(r_i)\right]\right\},\end{aligned} \tag{14a}$$

$$\begin{aligned}\eta^B_{m^I_{II}}(r_i)=&\mp\frac{imk_0^2}{2}\sum_{n=m}^{\infty}\left\{n(n+1)[P_n^m(0)]^2\right\}\\&\times\left\{\frac{h_n^{(1)}(k_0r_i)}{k_0r_i}\sum_{n'=m}^{\infty}\left[\mathcal{C}^4_{(m,n')^I_{II}}(r_i)\right]\right.\\&\left.+\frac{j_n(k_0r_i)}{k_0r_i}\sum_{n'=m}^{\infty}\left[\mathcal{D}^4_{(m,n')^I_{II}}(r_i)\right]\right\},\end{aligned} \tag{14b}$$

$$\begin{aligned}\xi^A_{m^I_{II}}(r_i)=&\pm\frac{imk_0^2}{2}\begin{bmatrix}1-\delta_{m0}\\1+\delta_{m0}\end{bmatrix}\sum_{n=m}^{\infty}\left\{n(n+1)[P_n^m(0)]^2\right\}\\&\times\left\{\frac{\partial[r_ih_n^{(1)}(k_0r_i)]}{k_0r_i\partial r_i}\sum_{n'=m}^{\infty}\left[\pm\mathcal{C}^2_{(m,n')^I_{II}}(r_i)-\mathcal{C}^3_{(m,n')^I_{II}}(r_i)\right]\right.\\&\left.\frac{\partial[r_ij_n(k_0r_i)]}{k_0r_i\partial r_i}\sum_{n'=m}^{\infty}\left[\pm\mathcal{D}^2_{(m,n')^I_{II}}(r_i)-\mathcal{D}^3_{(m,n')^I_{II}}(r_i)\right]\right\},\end{aligned} \tag{14c}$$

$$\begin{aligned}\xi^B_{m^I_{II}}(r_i)=&\frac{ik_0^2}{2}\begin{bmatrix}1-\delta_{m0}\\1+\delta_{m0}\end{bmatrix}\sum_{n=m}^{\infty}\left[\frac{\partial P_n^m(0)}{\partial\theta}\right]^2\\&\times\left\{h_n^{(1)}(k_0r_i)\sum_{n'=m}^{\infty}\left[\mathcal{C}^1_{(m,n')^I_{II}}(r_i)\right]\right.\end{aligned}$$

$$+ j_n(k_0 r_i) \sum_{n'=m}^{\infty} \left[\mathcal{D}^1_{(m,n')^I_{II}}(r_i)\right]\Bigg\}$$
$$+ \frac{im^2 k_0^2}{2} \begin{bmatrix} 1-\delta_{m0} \\ 1+\delta_{m0} \end{bmatrix} \sum_{n=m}^{\infty} [P_n^m(0)]$$
$$\times \left\{ \frac{\partial[r i j_n(k_0 r_i)]}{k_0 r_i \partial r_i} \sum_{n'=m}^{\infty} \left[\mathcal{C}^4_{(m,n')^I_{II}}(r_i)\right] \right.$$
$$\left. + \frac{\partial[r_i h_n^{(1)}(k_0 r_i)]}{k_0 r_i \partial r_i} \sum_{n'=m}^{\infty} \left[\mathcal{D}^4_{(m,n')^I_{II}}(r_i)\right] \right\}, \tag{14d}$$

$$\chi_{m^I_{II}}(r_i) = \sum_{n=m}^{\infty} \left[b^i_{\substack{e \\ o}} mn \, \frac{n(n+1) j_n(k_0 r_i)}{k_0 r_i} \, P_n^m(0) \right], \tag{14e}$$

$$\tau_{m^I_{II}}(r_i) = \sum_{n=m}^{\infty} (1-\delta_n 0) \left[-a^i_{\substack{o \\ e}} mn \, j_n(k_0 r_i) \, \frac{\partial P_n^m(0)}{\partial \theta} \right.$$
$$\left. \mp b^i_{\substack{e \\ o}} mn \, m \, \frac{\partial[r i j_n(k_0 r_i)]}{k_0 r_i \partial r_i} P_n^m(0) \right], \tag{14f}$$

with the intermediate parameters $\mathcal{C}^i_{(m,n')^I_{II}}(r_i)$ and $\mathcal{D}^i_{(m,n')^I_{II}}(r_i)$ ($i = 1, 2, 3,$ and 4) defined as follows:

$$\mathcal{C}^1_{(m,n')^I_{II}}(r_i) = a^i_{\substack{o \\ e}} mn' \, n'(n'+1) P^m_{n'}(0) \int_0^{r_i} r' dr'$$
$$\times j_n(k_0 r') \, \frac{j_{n'}(k_0 r')}{k_0 r_i} \, \frac{1}{\sqrt{1 - p\left(\frac{r'}{a}\right)^2}}, \tag{15a}$$

$$\mathcal{C}^2_{(m,n')^I_{II}}(r_i) = a^i_{\substack{o \\ e}} mn' \, m P^m_{n'}(0) \int_0^{r_i} r' dr'$$
$$\times \frac{j_n(k_0 r')}{k_0 r'} \, \frac{\partial[r' j_{n'}(k_0 r')]}{k_0 r' \partial r'} \sqrt{1 - p\left(\frac{r'}{a}\right)^2}, \tag{15b}$$

$$\mathcal{C}^3_{(m,n')^I_{II}}(r_i) = b^i_{\substack{e \\ o}} mn' \, \frac{\partial P^m_{n'}(0)}{\partial \theta} \int_0^{r_i} r' dr'$$
$$\times j_n(k_0 r') \frac{j_{n'}(k_0 r')}{k_0 r'} \sqrt{1 - p\left(\frac{r'}{a}\right)^2}, \tag{15c}$$

$$\mathcal{C}^4_{(m,n')^I_{II}}(r_i) = a^i_{\substack{o\\e}mn'}\, n'(n'+1)P^m_{n'}(0)\int_0^{r_i} r'dr' \times \frac{\partial[r'j_{n'}(k_0r')]}{k_0r'\partial r'}\,\frac{j_{n'}(k_0r')}{k_0r'}\,\frac{1}{\sqrt{1-p\left(\frac{r'}{a}\right)^2}}; \quad (15d)$$

and

$$\mathcal{D}^1_{(m,n')^I_{II}}(r_i) = a^i_{\substack{o\\e}mn'}\, n'(n'+1)P^m_{n'}(0)\int_{r_i}^{a} r'dr' \times h^{(1)}_n(k_0r')\frac{j_{n'}(k_0r')}{k_0r'}\,\frac{1}{\sqrt{1-p\left(\frac{r'}{a}\right)^2}}; \quad (16a)$$

$$\mathcal{D}^2_{(m,n')^I_{II}}(r_i) = a^i_{\substack{o\\e}mn'}\, mP^m_{n'}(0)\int_{r_i}^{a} r'dr' \times \frac{h^{(1)}_n(k_0r')}{k_0r'}\,\frac{\partial[r'j_{n'}(k_0r')]}{k_0r'\partial r'}\sqrt{1-p\left(\frac{r'}{a}\right)^2}, \quad (16b)$$

$$\mathcal{D}^3_{(m,n')^I_{II}}(r_i) = b^i_{\substack{e\\o}mn'}\,\frac{\partial P^m_{n'}(0)}{\partial\theta}\int_{r_i}^{a} r'dr' \times h^{(1)}_n(k_0r')\frac{j_{n'}(k_0r')}{k_0r'}\sqrt{1-p\left(\frac{r'}{a}\right)^2}, \quad (16c)$$

$$\mathcal{D}^4_{(m,n')^I_{II}}(r_i) = a^i_{\substack{o\\e}mn'}\, n'(n'+1)P^m_{n'}(0)\int_{r_i}^{a} r'dr' \times \frac{\partial[r'h^{(1)}_{n'}(k_0r')]}{k_0r'\partial r'}\,\frac{j_{n'}(k_0r')}{k_0r'}\,\frac{1}{\sqrt{1-p\left(\frac{r'}{a}\right)^2}}. \quad (16d)$$

In order to get the solution, each equation in Eq. (13) is split into two parts, namely the real part and the imaginary part, as follows:

$$Ar^m_{I\,II}\,\eta r^A_{m^I_{II}}(r_i) - Ai^m_{I\,II}\,\eta i^A_{m^I_{II}}(r_i) + Br^m_{I\,II}\,\eta r^B_{m^I_{II}}(r_i) - Bi^m_{I\,II}\,\eta i^B_{m^I_{II}}(r_i) = \chi r_{m^I_{II}}(r_i), \quad (17a)$$

$$Ar^m_{I\,II}\,\eta i^A_{m^I_{II}}(r_i) + Ai^m_{I\,II}\,\eta r^A_{m^I_{II}}(r_i) + Br^m_{I\,II}\,\eta i^B_{m^I_{II}}(r_i) + Bi^m_{I\,II}\,\eta r^B_{m^I_{II}}(r_i) = \chi i_{m^I_{II}}(r_i), \quad (17b)$$

$$Ar^{m}_{I\,II}\,\xi r^{A}_{m^{I}_{II}}(r_i) - Ai^{m}_{I\,II}\,\xi i^{A}_{m^{I}_{II}}(r_i) + Br^{m}_{I\,II}\,\xi r^{B}_{m^{I}_{II}}(r_i) - Bi^{m}_{I\,II}\,\xi i^{B}_{m^{I}_{II}}(r_i) = \tau r_{m^{I}_{II}}(r_i), \tag{17c}$$

$$Ar^{m}_{I\,II}\,\xi i^{A}_{m^{I}_{II}}(r_i) + Ai^{m}_{I\,II}\,\xi r^{A}_{m^{I}_{II}}(r_i) + Br^{m}_{I\,II}\,\xi i^{B}_{m^{I}_{II}}(r_i) + Bi^{m}_{I\,II}\,\xi r^{B}_{m^{I}_{II}}(r_i) = \tau i_{m^{I}_{II}}(r_i), \tag{17d}$$

where the letters r and i attached indicate the real and imaginary parts of the corresponding variables and coefficients, i.e.,

$$A^{m}_{I\,II} = Ar^{m}_{I\,II} + i\,Ai^{m}_{I\,II}, \tag{18a}$$

$$B^{m}_{I\,II} = Br^{m}_{I\,II} + i\,Bi^{m}_{I\,II}. \tag{18b}$$

To determine the unknown coefficients $Ar^{m}_{I\,II}$, $Ai^{m}_{I\,II}$ and $Br^{m}_{I\,II}$, $Bi^{m}_{I\,II}$ in the above equations, the least squares method is proposed as follows:

$$\left[\sigma^{r}_{\rho}\right]^2 = \sum_{i=1}^{N}\left[Ar^{m}_{I\,II}\,\eta r^{A}_{I\,II}(r_i) - Ai^{m}_{I\,II}\,\eta i^{A}_{m^{I}_{II}}(r_i) + Br^{m}_{I\,II}\,\eta r^{B}_{m^{I}_{II}}(r_i) - Bi^{m}_{I\,II}\,\eta i^{B}_{m^{I}_{II}}(r_i) - \chi\, r_{m^{I}_{II}}(r_i)\right]^2, \tag{19a}$$

$$\left[\sigma^{i}_{\rho}\right]^2 = \sum_{i=1}^{N}\left[Ar^{m}_{I\,II}\,\eta i^{A}_{m^{I}_{II}}(r_i) + Ai^{m}_{I\,II}\,\eta r^{A}_{m^{I}_{II}}(r_i) + Br^{m}_{I\,II}\,\eta i^{B}_{m^{I}_{II}}(r_i) + Bi^{m}_{I\,II}\,\eta r^{B}_{m^{I}_{II}}(r_i) - \chi\, i_{m^{I}_{II}}(r_i)\right]^2, \tag{19b}$$

$$\left[\sigma^{r}_{\phi}\right]^2 = \sum_{i=1}^{N}\left[Ar^{m}_{I\,II}\,\xi r^{A}_{m^{I}_{II}}(r_i) - Ai^{m}_{I\,II}\,\xi i^{A}_{m^{I}_{II}}(r_i) + Br^{m}_{I\,II}\,\xi r^{B}_{m^{I}_{II}}(r_i) - Bi^{m}_{I\,II}\,\xi i^{B}_{m^{I}_{II}}(r_i) - \tau r_{m^{I}_{II}}(r_i)\right]^2, \tag{19c}$$

$$\left[\sigma^{i}_{\phi}\right]^2 = \sum_{i=1}^{N}\left[Ar^{m}_{I\,II}\,\xi i^{A}_{m^{I}_{II}}(r_i) + Ai^{m}_{I\,II}\,\xi r^{A}_{m^{I}_{II}}(r_i) + Br^{m}_{I\,II}\,\xi i^{B}_{m^{I}_{II}}(r_i) + Bi^{m}_{I\,II}\,\xi r^{B}_{m^{I}_{II}}(r_i) - \tau i_{m^{I}_{II}}(r_i)\right]^2, \tag{19d}$$

where $\left[\sigma^{r}_{\rho}\right]^2$, $\left[\sigma^{i}_{\rho}\right]^2$, $\left[\sigma^{r}_{\phi}\right]^2$, and $\left[\sigma^{i}_{\phi}\right]^2$ stand for the error squares of Eqs. (17a), (17b), (17c), and (17d) separately. Therefore, the global

error square is the sum of (19a), (19b), (19c), and (19d), i.e.,

$$\sigma^2_{\text{global}} = \left[\sigma^r_\rho\right]^2 + \left[\sigma^i_\rho\right]^2 + \left[\sigma^r_\phi\right]^2 + \left[\sigma^i_\phi\right]^2. \tag{20}$$

To minimize the global error square, we enforce its derivatives with respect to $Ar^m_{\substack{I\\II}}$, $Ai^m_{\substack{I\\II}}$, $Br^m_{\substack{I\\II}}$ and $Bi^m_{\substack{I\\II}}$ to be zero as follows:

$$\frac{\partial \sigma^2_{\text{global}}}{\partial Ar^m_{\substack{I\\II}}} = 0, \tag{21a}$$

$$\frac{\partial \sigma^2_{\text{global}}}{\partial Ai^m_{\substack{I\\II}}} = 0, \tag{21b}$$

$$\frac{\partial \sigma^2_{\text{global}}}{\partial Br^m_{\substack{I\\II}}} = 0, \tag{21c}$$

$$\frac{\partial \sigma^2_{\text{global}}}{\partial Bi^m_{\substack{I\\II}}} = 0. \tag{21d}$$

From Eqs. (21a), (21b), (21c), and (21d), we obtain the following solutions:

$$\begin{bmatrix} Ar^m_{\substack{I\\II}} \\ Ai^m_{\substack{I\\II}} \\ Br^m_{\substack{I\\II}} \\ Bi^m_{\substack{I\\II}} \end{bmatrix} = \begin{bmatrix} \Phi^1_{m^I_{II}} \\ \Phi^2_{m^I_{II}} \\ \Psi^1_{m^I_{II}} \\ \Psi^2_{m^I_{II}} \end{bmatrix} \begin{bmatrix} \Gamma_{m^I_{II}} & 0 & \Omega^1_{m^I_{II}} & \Omega^2_{m^I_{II}} \\ 0 & \Gamma_{m^I_{II}} & -\Omega^2_{m^I_{II}} & \Omega^1_{m^I_{II}} \\ \Omega^1_{m^I_{II}} & -\Omega^2_{m^I_{II}} & \Upsilon_{m^I_{II}} & 0 \\ \Omega^2_{m^I_{II}} & \Omega^1_{m^I_{II}} & 0 & \Upsilon_{m^I_{II}} \end{bmatrix}^{-1} \tag{22}$$

where

$$\Gamma_{m^I_{II}} = \sum_{i=1}^{N} \left\{ \left[\eta r^A_{m^I_{II}}(r_i)\right]^2 + \left[\eta i^A_{m^I_{II}}(r_i)\right]^2 + \left[\xi r^B_{m^I_{II}}(r_i)\right]^2 + \left[\xi i^A_{m^I_{II}}(r_i)\right]^2 \right\}, \tag{23a}$$

$$\Upsilon_{m^I_{II}} = \sum_{i=1}^{N} \left\{ \left[\eta r^B_{m^I_{II}}(r_i)\right]^2 + \left[\eta r^B_{m^I_{II}}(r_i)\right]^2 + \left[\xi r^B_{m^I_{II}}(r_i)\right]^2 + \left[\xi i^B_{m^I_{II}}(r_i)\right]^2 \right\}, \tag{23b}$$

$$\Omega^1_{m^I_{II}} = \sum_{i=1}^{N}\Big[\eta r^A_{m^I_{II}}(r_i)\eta r^B_{m^I_{II}}(r_i) + \eta i^A_{m^I_{II}}(r_i)\eta i^B_{m^I_{II}}(r_i) + \xi r^A_{m^I_{II}}(r_i)\xi r^B_{m^I_{II}}(r_i) + \xi i^A_{m^I_{II}}(r_i)\xi r^B_{m^I_{II}}(r_i)\Big], \quad (23c)$$

$$\Omega^2_{m^I_{II}} = \sum_{i=1}^{N}\Big[-\eta r^A_{m^I_{II}}(r_i)\eta i^B_{m^I_{II}}(r_i) + \eta i^A_{m^I_{II}}(r_i)\eta r^B_{m^I_{II}}(r_i) - \xi r^A_{m^I_{II}}(r_i)\xi i^B_{m^I_{II}}(r_i) + \xi i^A_{m^I_{II}}(r_i)\xi r^B_{m^I_{II}}(r_i)\Big], \quad (23d)$$

$$\Phi^1_{m^I_{II}} = \sum_{i=1}^{N}\Big[\eta r^A_{m^I_{II}}(r_i)\chi r_{m^I_{II}}(r_i) + \eta i^A_{m^I_{II}}(r_i)\chi i_{m^I_{II}}(r_i) + \xi r^A_{m^I_{II}}(r_i)\tau r_{m^I_{II}}(r_i) + \xi i^A_{m^I_{II}}(r_i)\tau i_{m^I_{II}}(r_i)\Big], \quad (23e)$$

$$\Phi^2_{m^I_{II}} = \sum_{i=1}^{N}\Big[\eta r^A_{m^I_{II}}(r_i)\chi i_{m^I_{II}}(r_i) - \eta i^A_{m^I_{II}}(r_i)\chi r_{m^I_{II}}(r_i) + \xi r^A_{m^I_{II}}(r_i)\tau i_{m^I_{II}}(r_i) - \eta i^A_{m^I_{II}}(r_i)\tau r_{m^I_{II}}(r_i)\Big], \quad (23f)$$

$$\Psi^1_{m^I_{II}} = \sum_{i=1}^{N}\Big[\eta r^B_{m^I_{II}}(r_i)\chi r_{m^I_{II}}(r_i) + \eta i^B_{m^I_{II}}(r_i)\chi i_{m^I_{II}}(r_i) + \xi r^B_{m^I_{II}}(r_i)\tau r_{m^I_{II}}(r_i) + \xi i^B_{m^I_{II}}(r_i)\tau i_{m^I_{II}}(r_i)\Big], \quad (23g)$$

$$\Psi^2_{m^I_{II}} = \sum_{i=1}^{N}\Big[\eta r^B_{m^I_{II}}(r_i)\xi i_{m^I_{II}}(r_i) - \eta i^B_{m^I_{II}}(r_i)\chi r_{m^I_{II}}(r_i) + \xi r^B_{m^I_{II}}(r_i)\tau i_{m^I_{II}}(r_i) - \xi i^B_{m^I_{II}}(r_i)\tau r_{m^I_{II}}(r_i)\Big]. \quad (23h)$$

The number N used in (23) denotes the point number of the least squares fitting, subject to the requirement of accuracy. Once they are obtained, Ar^m_{II}, Ai^m_{II}, Br^m_{II} and Bi^m_{II}, A^m_{II} and B^m_{II} can be easily obtained from (18a) and (18b).

4. Scattered Electromagnetic Fields

After obtaining the coefficients $A^m_{I\ II}$ and $B^m_{I\ II}$, we can further derive the scattered electromagnetic fields by substituting (11) together with (18) into (7).

The scattered electric field is therefore obtained as

$$\boldsymbol{E}^s_{I\ II} = \sum_{n=1}^{\infty}\sum_{m=0}^{n}\left[A^s_{\substack{o\\e}mn}\,\boldsymbol{M}^{(1)}_{\substack{o\\e}mn} + B^s_{\substack{o\\e}mn}\,\boldsymbol{N}^{(1)}_{\substack{o\\e}mn}\right], \tag{24}$$

where the subscript (1) denotes that the spherical Bessel functions $z_n(kr)$ in the vector wave functions take the form of the spherical Hankel functions of the first kind $h^{(1)}_n(kr)$, and the scattering coefficients are given by

$$\begin{aligned}
\mathcal{A}^s_{\substack{o\\e}mn} =& B_{m^I_{II}}\frac{ik_0}{2}\,C_{mn}\begin{bmatrix}1-\delta_{m0}\\1+\delta_{m0}\end{bmatrix}\frac{\partial P^m_n(0)}{\partial\theta}\sum_{n'=m}^{\infty}a^i_{\substack{o\\e}mn}\,P^m_{n'}(0)n'(n'+1)\\
&\times\int_0^a\frac{j_{n'}(k_0r')j_n(k_0r')}{\sqrt{1-p\left(\frac{r'}{a}\right)^2}}\,dr', \qquad (25a)\\
\mathcal{B}^s_{\substack{o\\e}mn} =& \pm B_{m^I_{II}}\frac{i}{2}\,C_{mn}\,mP^m_n(0)\sum_{n'=m}^{\infty}a^i_{\substack{o\\e}mn}\,P^m_{n'}(0)n'(n'+1)\\
&\times\int_0^a\frac{\partial[r'j_{n'}(k_0r')]}{\partial r'}\,\frac{j_n(k_0r')}{\sqrt{1-p\left(\frac{r'}{a}\right)^2}}\,dr'\\
&+A_{m^I_{II}}\begin{bmatrix}1+\delta_{m0}\\1-\delta_{m0}\end{bmatrix}n(n+1)P^m_n(0)\\
&\times\sum_{n'=m}^{\infty}\left\{\pm a^i_{\substack{o\\e}mn}\,mP^m_{n'}(0)\int_0^a dr'\,\frac{\partial[r'j_{n'}(k_0r')]}{k_0r'\partial r'}\right.\\
&\times j_n(k_0r')\sqrt{1-p\left(\frac{r'}{a}\right)^2}-b^i_{\substack{o\\e}mn}\,\frac{\partial P^m_{n'}(0)}{\partial\theta}\\
&\left.\times\int_0^a dr'j_{n'}(k_0r')j_n(k_0r')\sqrt{1-p\left(\frac{r'}{a}\right)^2}\right\}. \qquad (25b)
\end{aligned}$$

5. BACKSCATTERING CROSS SECTION

The backscattering cross section is defined as

$$\sigma = \lim_{r\to\infty}\left[4\pi r^2 \frac{|E^s|^2}{|E^i|^2}\right], \tag{26}$$

in which $|E^s|$ and $|E^i|$ are the amplitudes of scattered and incident electric fields, respectively. The normalized backscattering cross section for a perfectly conducting circular disk is defined as

$$\sigma_{\text{normal}} = \frac{\sigma}{\pi a^2}\,, \tag{27}$$

where a is the radius of the disk.

6. NUMERICAL DISCUSSION

With the formulation developed in the previous section, we have performed the computation of the monostatic RCS's for a disk of 2 inch and 4.5 inch radii, and the normalized monostatic RCS's at a frequency of 10 GHz for cases where $k_0 a = 8.59$ and 9.45. For all the cases computed, the thickness of the perfectly conducting disk is considered as infinitesimal, and the RCS computation is performed for both parallel and perpendicular polarizations. At the same time, the modification constant p is taken as 0.99 and the point number of the least square fitting $N = 20$.

In order to check the effectiveness of the present method based on the modified PO current, the numerical data for all the cases mentioned above are compared with the published measured data and the results obtained using the PO method.

Fig. 2 and Fig. 3 show the angular behaviors of the backscattering cross sections of circular disks of radii 2 inch and 4.5 inch, respectively. In both these figures, part (a) corresponds to the parallel polarization incident wave, while part (b) corresponds to the perpendicular polarization case. It can be seen from the figures that the results obtained from the present method agree with the measured results much better than those of PO method throughout the whole range of the backscattering angle from -90 to 90 degrees. Especially for the RCS's shown in the Fig. 2(b) of the 2-inch disk illuminated by the perpendicular polarization incident wave, our method produces very good results close to

the experimental data. It can be observed that in the low range from around ± 60 degrees to ± 90 degrees, the RCS level obtained from the PO method for the small disk drops below minus fifty dB which is far away from the measure results, while the result of the present hybrid method still agrees reasonably well with the measured data. Since it is well known that the PO method has an inherent weakness when applied to calculate the scattering of the relatively small object, it is of no surprise to see such phenomena. Meanwhile, this also indicates the great improvement introduced by the hybrid method that is newly proposed based on e modified PO current.

When computing the RCS for the large disk with the radius 4.5 inch, the same point number of the least square fitting is adopted which means the computation time has almost not increased with the increased disk size. It is observed from Fig. 3 that the result of the hybrid method still agrees well with the measured result. It is well-known that the Method of Moment fails when the object dimension becomes very large. The method can deal with the large disk; especially, the speed of the analysis can be almost retained. This indicates another advantage of the new method presented.

Similar comparisons are also shown in Fig. 4 and Fig. 5 with the normalized backscattering cross sections for cases where $k_0 a = 8.59$ and 9.45 ($a/\lambda = 1.367$ and 1.5), respectively. The same parameters of a and f as those in the experiment are used for ease of comparison. The results of the hybrid method also agree well with the measured data especially for the low angular behavior of RCS's for the perpendicular polarization incident wave. Phenomena similar to those of the 2 inch disk are observed.

7. CONCLUSIONS

In this paper, a novel hybrid method has been developed for the analysis of the classical electromagnetic scattering by a perfectly conducting circular disk. It provides an alternative way to solve electromagnetic scattering problems. This method combines the eigenfunction expansion technique, the model matching technique, the least squares fitting method, and the dyadic Green's function technique. With this hybrid technique, the unknown scattering coefficients of the expanded eigenfunctions in the expression of the scattered fields are derived in a compact matrix form in this paper. Both TE- and TM-mode incident plane waves are considered in the analysis. After the scattering

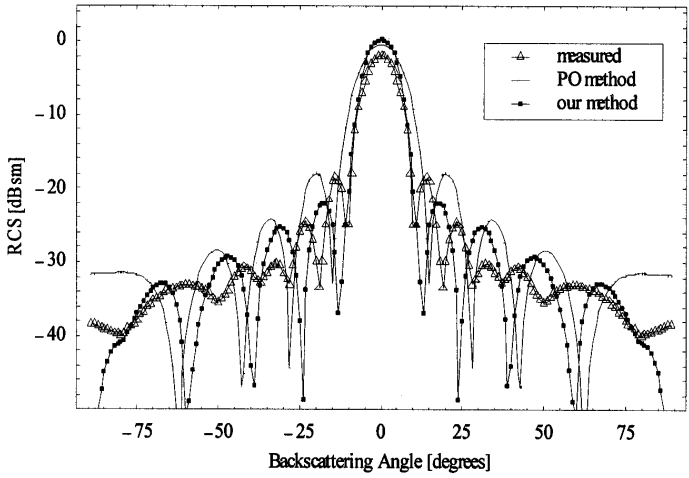

(a) Parallel polarization

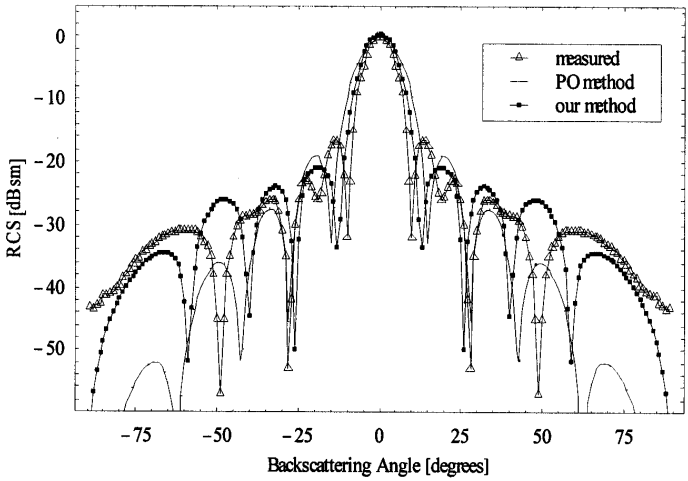

(b) Perpendicular polarization

Figure 2. Monostatic RCS patterns of a circular disk ($a = 2$ inch and $f = 10$ GHz) from (i) the measurement, (ii) the PO method, and (iii) our method.

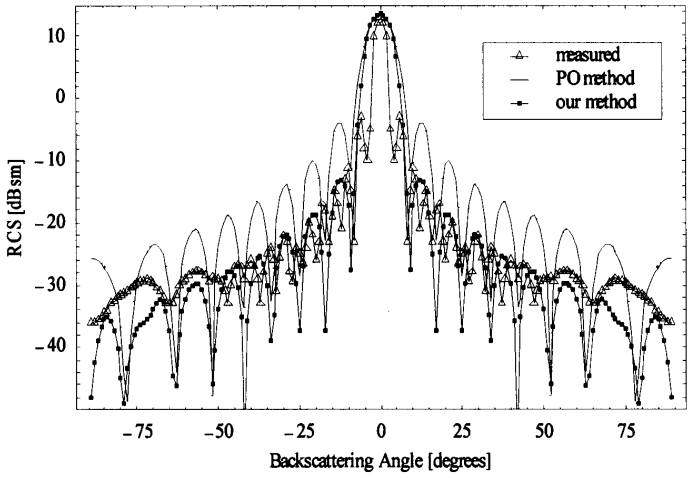

(a) Parallel polarization

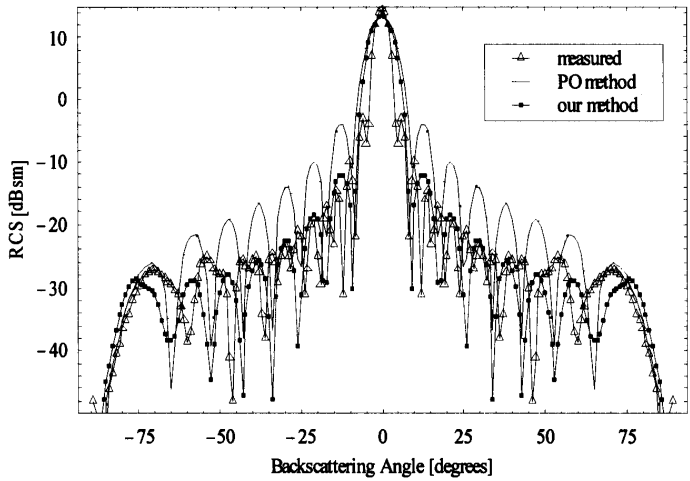

(b) Perpendicular polarization

Figure 3. Monostatic RCS patterns of a circular disk ($a = 4.5$ inch and $f = 10$ GHz) from (i) the measurement, (ii) the PO method, and (iii) our method.

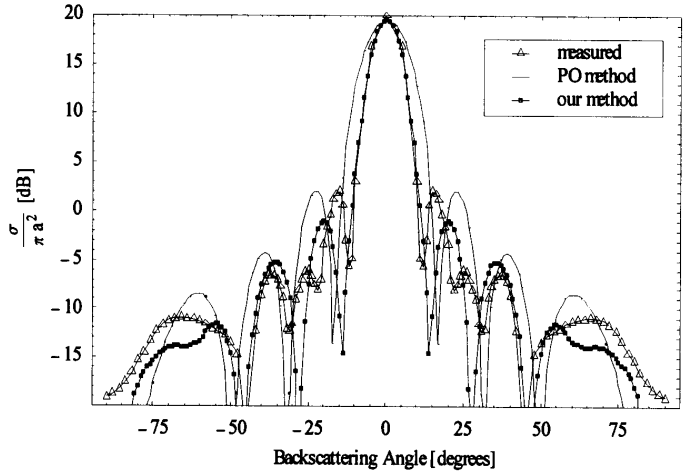

(a) Parallel polarization

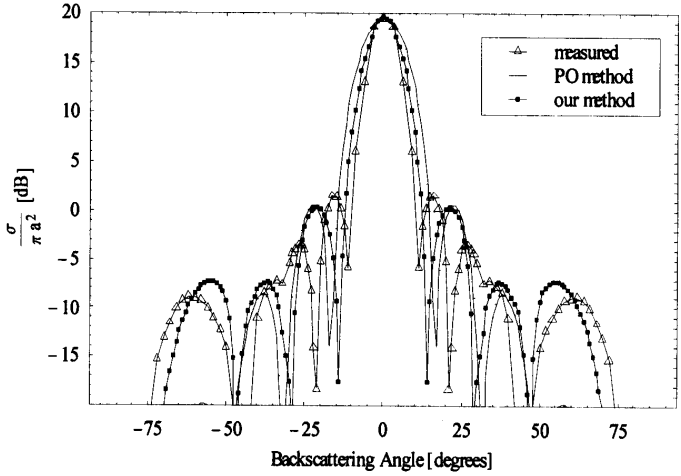

(b) Perpendicular polarization

Figure 4. Normalized monostatic RCS patterns of a circular disk ($k_0a = 9.45$ and $f = 10$ GHz) from (i) the measurement, (ii) the PO method, and (iii) our method.

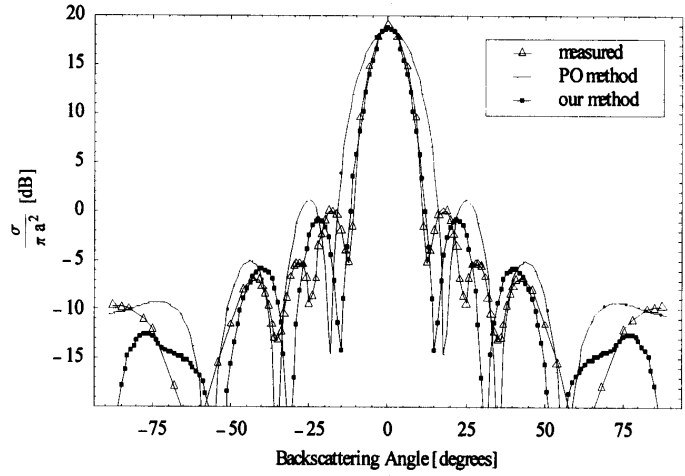

(a) Parallel polarization

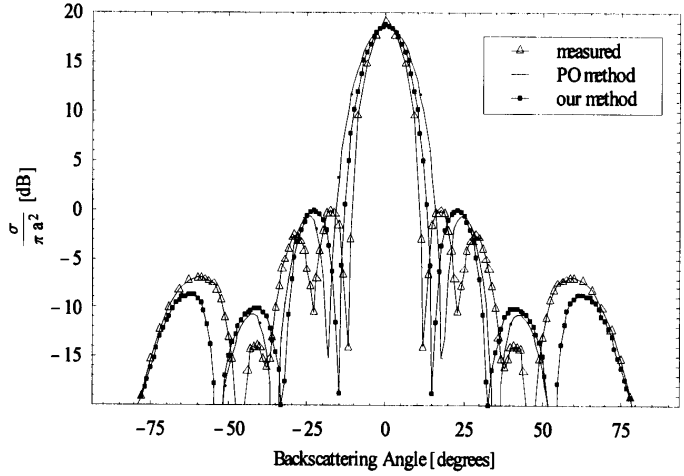

(b) Perpendicular polarization

Figure 5. Normalized monostatic RCS patterns of a circular disk ($k_0 a = 8.59$ and $f = 10$ GHz) from (i) the measurement, (ii) the PO method, and (iii) our method.

coefficients are successfully obtained in a closed form, numerical computation of the radar cross sections of the perfectly conducting disk has been carried out. The results are compared with some published measured data and the results obtained using the POmethod. A reasonably good agreement between the experimental data and our computed results is shown in the comparison. It is also shown that similar to the Method of Moments, the hybrid method achieves a higher accuracy than that of the conventional PO method. At the same time, it can be applied to a relatively large disk without considerably increasing the computation time. With this method, computational speed can be controlled by choosing appropriate number and distribution of the least squares points, subject to the required accuracy.

ACKNOWLEDGEMENT

The research work carried out here is supported by a research grant No. RP950646 from the National University of Singapore.

REFERENCES

1. Duan, D-W, Y. Rahmat-Samii, and J. P. Mahon, "Scattering from a circular disk: A comparative study of PTD and GTD techniques," *Proc. IEEE,* Vol. 79, No. 10, 1472–1480, 1991.
2. Rahmat-Samii, Y., "Reflector antennas," in *Antenna Handbook,* Lo, Y. T., and Lee, S. W., Eds., chapter 15, Van Nostrand-Reinhold Company, New York, 1988.
3. Ufimtsev, P. Y., "Method of edge waves in the physical theory of diffraction," *Izd-Vo Sovyetskoye Radio,* Translation by US Air Force Foreign Technology Division, 1–1154, 1962.
4. Ando, M., "Radiation pattern analysis of reflector antennas," Tech. report, Aircraft Division Northrop Corp., AFA1-TR-73-296, 1974.
5. Mitzner, K. M., "Incremental length diffraction coefficients," Tech. report, Aircraft Division Northrop Corp., AFA1-TR-73-296, 1974.
6. Michaeli, A., "Equivalent edge currents for arbitrary aspects of observation," *IEEE Trans. Antennas Propagat.,* Vol. AP-43, No. 3, 252–258, 1984, also see erratum, Vol. AP-33, 227, 1985.
7. Michaeli, A., "Elimination of infinities in equivalent edge currents-Part I: Fringe current components," *IEEE Trans. Antennas Propagat.,* Vol. AP-33, No. 1, 112–114, 1985.

8. Knott, E. F., "The relationsh between Mitzner's ILDC and Michaeli's equivalent currents," *IEEE Trans. Antennas Propagat.,* Vol. AP-33, No. 7, 912–918, 1986.
9. Meixner, J., and W. Andrejewski, "Strenge theorie der Beugung ebener elektromagnetischer Wllen ebenen Schirm," *Ann. Physik.,* Vol. 7, 157–168, 1950.
10. Keller, J. B., "Diffraction by an aperture," *J. Appl. Phys.,* Vol. 28, 426–444, 1957.
11. Keller, J. B., "Geometrical theory of diffraction," *J. Opt. Soc. Amer.,* Vol. 52, 116–130, 1962.
12. James, G. L., *Geometrical Theory of Diffraction for Electromagnetic Waves,* Peter Perengrinus, Ltd., Stevenge, UK, 1976.
13. Balanis, C. A., *Advanced Enginering Electromagnetics,* John Wiley & Sons, New York, 1989.
14. Kouyoumjian, R. G., and P. H. Pathak, "A uniform geometrical theory of diffraction of an edge in a perfectly conducting surface," *Proc. IEEE,* Vol. 62, 14480–1461, 1974.
15. Ahluwalia, D. S., R. M. Lewis, and J. Boersma, "Uniform asymptotic theory of diffraction by a plane screen," *SIAM J. Appl. Math.,* Vol. 16, 783–807, 1968.
16. Lee, S. W., and G. A. Deschamps, "A uniform asymptotic theory of electromagnetic diffraction by a curved wedge," *IEEE Trans. Antennas Propagat.,* Vol. AP-24, 25–34, 1976.
17. Bechtel, M. E., "Application of geometric diffraction theory to scattering from cones and disks," *Proc. IEEE,* Vol. 53, 877–882, 1965.
18. Ryan Jr., C. E., and L. Peters, Jr., "Evaluation of edge-diffracted fields including equivalent currents for the caustic regions," *IEEE Trans. Antennas Propagat.,* Vol. AP-17, No. 3, 292-299, 1969.
19. Knott, E. F., T. B. A. Senior, and P. L. E. Uslenghi, "High frequency backscattering from a metallic disk," *Proc. Inst. Elec. Eng.,* Vol. 118, No. 12, 1736–1742, 1971.
20. Marsland, D. P., C. A. Balanis, and S. A. Brumley, "Higher order diffractions from a circular disk," *IEEE Trans. Antennas Propagat.,* Vol. AP-35, No. 12, 1436–1444, 1987.
21. Kaye, M., P. K. Murthy, and G. A. Thiele, "An iterative method for solving scattering problems," *IEEE Trans. Antennas Propagat.,* Vol. AP-33, 1272–1279, 1985.
22. Murthy, P. K., K. C. Hill, and G. A. Thiele, "A hybrid-iterative method for solving scattering problems," *IEEE Trans. Antennas Propagat.,* Vol. AP-34, No. 10, 1173–1180, 1986.

23. Morrison, J. A., and J. M. Cross, "Scattering of a plane electromagnetic wave by axisymmetric raindrops," *Bell Syst. Tech. J.,* Vol. 53, 955–1019, 1974.
24. Tai, C. T., *Dyadic Green's Functions in Electromagnetic Theory,* IEEE Press, Piscataway, New Jersey, 2nd edition, 1994.
25. Li, L. W., P. S. Kooi, M. S. Leong, and T. S. Yeo, "Electromagnetic dyadic Green's functions in spherically multilayered media," *IEEE Trans. Microwave Theory Tech.,* Vol. 42, No. 12, 2302–2310, Part A, 1994.
26. Harrington, R. F., *Time Harmonic Electromagnetic Fields,* McGraw-Hill, New York, 1961.
27. Harrington, R. F., *Field Computation by Moment Methods,* IEEE/Oxford University Press, New Jersey, 1995.